

Impact of Intra-Flow Interference on the Performance of 2D Multi-Hop Cooperative Network

Muddassar Hussain and Syed Ali Hassan, *Member, IEEE*

Abstract—A mathematical model is proposed to study the effects of intra-flow interference caused due to multi-packet propagation in a 2D cooperative opportunistic large array (OLA) network. Specifically, the outage probability of node is derived in the presence of interfering signals using the ratio distribution of generalized integer gamma random variables. The outage probability expression is used along with a Markov chain-based transmission model to quantify the state distribution probabilities, coverage of the network, and network throughput. The results show that the network performance is highly dependent on intra-flow interference especially at high signal-to-noise ratio (SNR). Moreover, the coverage of network can be improved by increasing SNR, array gain, and packet insertion rate.

I. INTRODUCTION

COOPERATIVE transmission (CT) has emerged as one of the successful techniques in wireless communication to overcome the effects of multipath fading by virtue of spatial diversity. CT offers significant advantages over conventional point-to-point communication that include energy-efficiency [1] and range extension [2], thereby making it highly desirable to be used in wireless sensor networks (WSNs). An effective and low-complexity physical layer CT scheme is opportunistic large array (OLA) where a group of radios opportunistically take part in transmitting the same message to another group of radios without any coordination within the group [3]. Since the inter-nodal coordination is not desirable in low-energy WSNs, OLA finds numerous applications pertaining to practical scenarios in WSNs such as structural health monitoring, vehicular networks, and smart-grid communication.

One important factor that degrades the performance of OLA networks is the intra-flow interference, i.e., the interference caused by simultaneous transmissions of different packets over different hops whereby all the transmissions use same channel. The impact of intra-flow interference on the performance of strip shaped OLA-based networks has been previously studied in [4] in which authors have analyzed network outage under *continuum* assumption that implies infinite node density (number of nodes per unit area) with a constant finite transmit power per unit area. However, this assumption may not be valid for finite density networks especially for the networks with low node density such as the 2D OLA network studied in [5]. Similarly, [6] carries some resemblance with this manuscript, where the interference effects in unicast barrage relay networks are studied using the analytical framework built in [7].

In this paper, we aim to investigate the impacts of intra-flow interference on the performance of a finite density OLA

network. For this purpose, we consider a two dimensional (2D) multihop OLA network with finite node density and mathematically model the interference caused by different levels due to multipacket transmissions at different hops. Specifically, we model the desired signal power and interference power appearing at a node as generalized integer gamma (GIG) random variables (RVs) and derive a closed-form expression of outage probability of a node using a ratio distribution. The expression of outage can then used to derive the hop outage and coverage probabilities as a function of node distribution, average signal-to-noise ratio (SNR), path loss exponent, packet insertion interval and interference tiers. The obtained results show a significant coverage degradation due to intra-flow interference. Moreover, a tradeoff is observed between the network throughput and coverage.

II. SYSTEM MODEL

Consider a 2D network topology shown in Fig. 1, where each level (or hop) consists of M nodes placed in a 2D geometry of $L \times H$ nodes as a rectangular region. Each node is a distance d apart from its adjacent node in both horizontal and vertical dimension, while the interhop distance is kept $M \times d$ to get a topology with non-overlapping hops. It is assumed that the nodes are half-duplex and use decode-and-forward (DF) mechanism for cooperative relaying. The nodes which successfully decode the received signal relay it to next level's nodes, therefore, these nodes are referred to as DF nodes and are shown as filled circles in Fig. 1. Hence the propagation of the message from source to destination is accomplished using cooperative multi-hop relaying. Furthermore, multiple packets traverse the network simultaneously from same source, which are denoted by ρ_m in Fig. 1, where m is the packet number and $m \in \mathbb{Z}^+$; \mathbb{Z}^+ is set of positive integers.

The source transmits a new packet after waiting R time slots, where $R \in \mathbb{Z}^+$. As multiple packets are transmitted simultaneously, the interference is caused at each receiving node. We denote the set of interfering levels whose transmissions create interference at the level n by \mathbb{I}_n . Assuming an extended 2D network, there exist infinite interfering levels, however, the interfering levels with appreciable level of average interference power are finite because the average interference power from interfering levels with large distance from the receiving level is negligible due to their huge path loss. Therefore, we only consider the interfering levels within T tiers of desired level, where $T \in \mathbb{Z}^+$. It should be noted that the all active (transmitting) levels are considered interfering for a receiving hop except its desired level. The active levels with

The authors are with National University of Sciences and Technology (NUST), Pakistan (email: {muddassar.hussain, ali.hassan}@seecs.edu.pk).

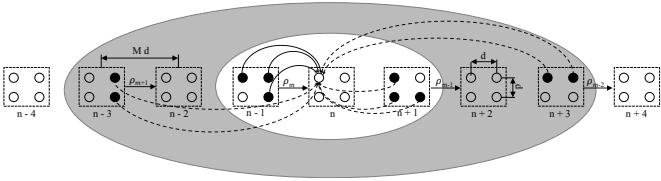


Fig. 1: The network topology for $M = 4$, $L = H = 2$, $R = 1$, and $T = 1, 2$.

respect to n^{th} receiving level is given by $n - 1 + (R + 1)i$, $i \in \{0, \pm 1, \pm 2, \dots\}$. An interference scenario for $R = 1$ is illustrated for a single node of level n in Fig. 1. The solid lines from DF nodes of level $n - 1$ denote the desired signal, whereas the dotted lines from the DF nodes of level $n + 1$, $n - 3$, and $n + 3$ show the interfering signals. The first tier of interference includes the interfering levels enclosed by inner unfilled ellipse, whereas second tier of interference includes outer filled ellipse. Thus, for $T = 1$, $\mathbb{I}_n = \{n + 1\}$, and for $T = 2$, $\mathbb{I}_n = \{n - 3, n + 1, n + 3\}$.

III. OUTAGE PROBABILITY

Assuming equal transmit power for each node, the signal-to-interference-plus-noise ratio (SINR) of p^{th} node at level n is given as

$$\gamma_p^{(n)} = \frac{\sum_{q \in \mathbb{N}_{n-1}} g_{p,q} \|x_p - x_q\|^{-\beta}}{\sum_{l \in \mathbb{I}_n} \sum_{k \in \mathbb{N}_l} g_{p,k} \|x_p - x_k\|^{-\beta + \bar{\gamma}^{-1}}}, \quad (1)$$

where \mathbb{N}_l represents the set of DF nodes at level l . The symbol $g_{k,j}$ denotes the channel gain from node k to node j , while x_j denotes the coordinates of node j in Euclidean geometry, where $\|\cdot\|$ is Euclidean norm. Assuming Rayleigh flat fading channel, the channel gains follow exponential distribution with unit mean. The $\bar{\gamma} = P/N_0$, where P is the transmit power and N_0 is the one-sided power spectral density of the additive white Gaussian noise (AWGN), and β denotes the path loss exponent. It can be noticed that the numerator and the denominator in (1) contain the sum of exponential RVs. In the following lemma, the PDF of the sum of exponential RVs will be provided.

Lemma 1. Let RV $Z := \sum_{i=1}^N X_i$, where $X_i, \forall i$ are independent non-identically distributed (i.n.i.d) Erlang RVs¹ with respective rate and shape parameter λ_i and k_i such that $\lambda_i \neq \lambda_j$, for $i \neq j, \forall i, j = 1, 2, \dots, N$. The RV Z then follows a generalized integer gamma (GIG) distribution and has following PDF

$$f_Z(x, \mathbf{K}, \boldsymbol{\lambda}) = \sum_{i=1}^N \frac{\lambda_i^{k_i}}{\exp(x\lambda_i)} \sum_{j=1}^{k_i} \frac{(-1)^{k_i-j} x^{j-1} \alpha_{ij}(\mathbf{K}, \boldsymbol{\lambda}, N)}{(j-1)!} u(x),$$

where

$$\alpha_{ij}(\mathbf{K}, \boldsymbol{\lambda}, N) = \sum_{a_1 + \dots + a_N = k_i - j} \prod_{b=1}^N \left[\binom{k_b + a_b - 1}{a_b} \frac{\lambda_b^{k_b}}{(\lambda_b - \lambda_i)^{k_b + a_b}} \right],$$

where $\boldsymbol{\lambda} = [\lambda_1, \lambda_2, \dots, \lambda_N]$, $\mathbf{K} = [k_1, k_2, \dots, k_N]$ and $u(x)$ is unit step function.

¹Note that each Erlang RV is a sum of independent exponential RVs with same parameter λ , i.e., $X_i = \sum_{j=1}^{k_i} Y_j$, where $Y_j \sim \text{Exp}(\lambda_i), \forall j$.

Using Lemma 1, we denote (1) as $\gamma_p^{(n)} = S/(I + \bar{\gamma}^{-1})$. The RVs $S \sim \text{GIG}(\mathbf{K}, \boldsymbol{\eta})$ and $I \sim \text{GIG}(\mathbf{N}, \boldsymbol{\nu})$, where $\mathbf{K} = [k_1, k_2, \dots, k_{N_S}]$, $\mathbf{N} = [n_1, n_2, \dots, n_{N_I}]$, $\boldsymbol{\eta} = [\eta_1, \eta_2, \dots, \eta_{N_S}]$, and $\boldsymbol{\nu} = [\nu_1, \nu_2, \dots, \nu_{N_I}]$. It should be noticed that k_i denotes the number of exponential RVs of i^{th} group in sum S having same rate parameter η_i , which is the path loss (i.e., distance raised to power β). Similarly, n_i is the number of exponential RVs of i^{th} group in sum I having same rate parameter ν_i . The N_S and N_I denote the total number of Erlang RVs with distinct rate parameter whose sum yield S and I , respectively. We now consider following theorem.

Theorem 1. The success probability of the receiving node p at level n is given as

$$\Psi_p^{(n)} = \sum_{i=1}^{N_S} \sum_{j=1}^{k_i} \sum_{\ell=1}^{N_I} \sum_{m=1}^{n_\ell} \left[\frac{(-1)^{k_i+n_\ell-j-m} \eta_i^{k_i-j} \nu^{n_\ell} \theta_{ij} \phi_{\ell m}}{\exp(\eta_i \tau \bar{\gamma}^{-1})} \right. \\ \left. \times \sum_{\xi=0}^{j-1} \frac{(\eta_i \tau)^\xi}{\bar{\gamma}^{\xi+m} \xi!} \psi \left(m, \xi + m + 1, \frac{\nu_\ell + \eta_i \tau}{\bar{\gamma}} \right) \right], \quad (2)$$

where $\psi(\cdot, \cdot, \cdot)$ is Kummer's confluent hypergeometric function and τ is the modulation dependent SINR decoding threshold. The $\theta_{ij} = \alpha_{ij}(\mathbf{K}, \boldsymbol{\eta}, N_S)$, and $\phi_{\ell m} = \alpha_{\ell m}(\mathbf{N}, \boldsymbol{\nu}, N_I)$.

Proof. The success probability of node p at level n is defined as $\Psi_p^{(n)} = \mathbb{P}(\gamma_p^{(n)} > \tau) = \mathbb{P}\left(\frac{S}{I + \bar{\gamma}^{-1}} > \tau\right)$. We get following equation after some mathematical manipulations

$$\Psi_p^{(n)} = \int_0^\infty \int_{\tau(y + \bar{\gamma}^{-1})}^\infty f_S(x) f_I(y) dx dy, \quad (3)$$

where $f_S(x) = f_Z(x, \mathbf{K}, \boldsymbol{\eta})$ and $f_I(y) = f_Z(y, \mathbf{N}, \boldsymbol{\nu})$. By substituting expression of $f_S(x)$ in (3), we get

$$\Psi_p^{(n)} = \sum_{i=1}^{N_S} \sum_{j=1}^{k_i} \frac{(-1)^{k_i-j} \theta_{ij}}{\eta_i^{k_i} (j-1)!} \int_0^\infty f_I(y) \int_{\tau(y + \bar{\gamma}^{-1})}^\infty \frac{x^{j-1}}{\exp(x\eta_i)} dx dy.$$

After solving the integral involving variable x in above equation, and substituting $f_I(y)$, we get

$$\Psi_p^{(n)} = \sum_{i=1}^{N_S} \sum_{j=1}^{k_i} \sum_{\ell=1}^{N_I} \sum_{m=1}^{n_\ell} \left[\frac{(-1)^{k_i+n_\ell-j-m} \eta_i^{k_i-j} \nu^{n_\ell} \theta_{ij} \phi_{\ell m}}{\exp(\eta_i \tau \bar{\gamma}^{-1}) (m-1)!} \right. \\ \left. \times \sum_{\xi=0}^{j-1} \frac{(\eta_i \tau)^\xi}{\xi!} \int_0^\infty \exp(-(\nu_\ell + \eta_i \tau)y) y^{m-1} (y + \bar{\gamma}^{-1})^\xi dy \right].$$

After solving the integral above, expression of success probability is obtained, which is given in (2). ■

For high SINR case (i.e., $\bar{\gamma} \rightarrow \infty$), the success probability is simply given by complementary cumulative density function (CCDF) of ratio of GIG RVs S and I , i.e., $\Psi_p^{(n)} = \mathbb{P}\left(\frac{S}{I} > \tau\right)$. Therefore, success probability for high SINR case is given as

$$\Psi_p^{(n)} = \sum_{i=1}^{N_S} \sum_{j=1}^{k_i} \sum_{\ell=1}^{N_I} \sum_{m=1}^{n_\ell} \left[\frac{(-1)^{k_i+n_\ell-j-m} \eta_i^{k_i-j} \nu^{n_\ell} \theta_{ij} \phi_{\ell m}}{(m-1)!} \right. \\ \left. \times \sum_{\xi=0}^{j-1} \frac{(\eta_i \tau)^\xi (\xi + m - 1)!}{\xi! (\nu_\ell + \eta_i \tau)^{\xi+m}} \right]. \quad (4)$$

It should be noted that the outage probability is simply given as $\Phi_p^{(n)} = 1 - \Psi_p^{(n)}$. In the sequel, we will use the expression of the success probability to find the hop outage probability.

Algorithm 1 Recursive Solver

- 1: Initialize $i = 0$, $\mathbf{Q}_n^{(0)} = \mathbf{0}$, $\pi_m^{(0)}(0) = 1/(2^M - 1)$, and $\pi_m^{(0)}(n) = 0, \forall n = 1, 2, \dots, H, \forall m \in \mathcal{X}$
 - 2: $i \leftarrow i + 1$
 - 3: **for** each hop n **do**
 - 4: Find $\mathbf{Q}_n^{(i)}$ from (5) using $\pi_m^{(i-1)}(\ell), \ell \in \mathbb{I}_n$
 - 5: Update $\pi_m^{(i)}(n)$ using (6)
 - 6: **end for**
 - 7: **if** $\|\mathbf{Q}_n^{(i)} - \mathbf{Q}_n^{(i-1)}\|_F \leq \epsilon, \forall n$ **then**
 - 8: Stop iteration
 - 9: **else**
 - 10: Go to step 2
 - 11: **end if**
-

IV. THE MARKOV MODEL

In this section, we present a mathematical model based upon discrete-time Markov chain to study the multi-hop transmissions in the OLA network.

The state of the node k at level n is denoted by a binary indicator function $\mathcal{I}_k^{(n)}$, which is 1 if k^{th} node is DF, and is 0 otherwise.

The state of level n can be represented as $\mathcal{S}_n = [\mathcal{I}_1^{(n)}, \mathcal{I}_2^{(n)}, \dots, \mathcal{I}_M^{(n)}]$, where $\mathcal{S}_n \in \mathcal{S}$; and $\mathcal{S} = \{0\} \cup \mathcal{X}$. The \mathcal{X} is a finite transient irreducible state space encompassing all the transient states, i.e., the states in which at least one node is DF. The symbol 0 denotes the absorbing state, i.e., the state in which all nodes of a level fail to decode. Ignoring transitions to/from the absorbing state, we can have transition probability matrix \mathbf{Q} , which has elements given as

$$q_{ij} = \sum_{s \in \mathcal{S}_n} \prod_{\substack{\ell \in \mathbb{I}_n \\ m = s_\ell}} \pi_m(\ell) p_{ij|s}, \quad (5)$$

where \mathcal{S}_n is state space containing all possible permutations of states of interfering levels and $\pi_m(\ell)$ is the probability that interfering level ℓ is in state m ; $m \in \mathcal{S}$. The probability of absorbing state in terms of transient state probabilities is given as $\pi_0(n) = 1 - \sum_{j \in \mathcal{X}} \pi_j(n)$. The symbol $p_{ij|s}$ represents the transition probability from the state i to state j given the interfering state is s , where $s \in \mathcal{S}_n$ and $p_{ij|s} = \prod_{p \in \mathbb{N}_n^{(j)}} \Psi_{p|i,s}^{(n)} \prod_{q \in \bar{\mathbb{N}}_n^{(j)}} (1 - \Psi_{q|i,s}^{(n)})$. The symbols $\mathbb{N}_n^{(j)}$ and $\bar{\mathbb{N}}_n^{(j)}$ represent the set of DF and non-DF nodes, respectively, corresponding to state j at level n . The symbol $\Psi_{p|i,s}^{(n)}$ denotes the success probability of p^{th} node at level n given desired state is i and interfering state is s . Using (5), state distribution probabilities of level n are given as

$$\pi_j(n) = \sum_{i \in \mathcal{X}} \pi_i(n-1) q_{ij}, \quad (6)$$

where $j \in \mathcal{X}$. It can be noticed from (6) that the value of $\pi_m(\ell)$, $m \in \mathcal{S}$, $\ell \in \mathbb{I}_n$, should be known to evaluate value of $\pi_j(n)$. Unfortunately, a direct solution to (6) is prohibitive;

therefore, we propose a recursive algorithm for solving (6), which is given in Algorithm I. The symbol $\|\cdot\|_F$ represents

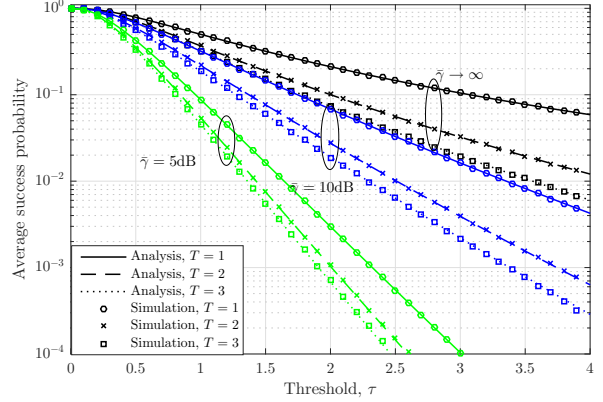


Fig. 2: The average success probability versus τ for different tiers of interference and $\bar{\gamma}$; $M = 3$, $L = 1$, $H = 3$, $d = 1m$, $R = 1$, and $\beta = 2$.

the Frobenius norm operator, H is maximum number of hops, and ϵ is a given tolerance.

V. RESULTS AND PERFORMANCE ANALYSIS

In this section, we analyze the performance of the finite density OLA networks with multi-packet insertion for various network parameters.

In Fig. 2, we compare the results of the average success probability at one hop for different values of T and $\bar{\gamma}$. For the results shown, we assume all the nodes of the interfering as well as desired levels are DF. The analytical results shown in the figure are obtained by using (2) and (4) for finite and infinitely large $\bar{\gamma}$, respectively. It can be noticed that analytical and simulation results match closely, thereby validating Theorem 1. It is evident from the figure that the success probability has an inverse monotonic relation with the τ . Moreover, if we compare the curves corresponding to different T and $\bar{\gamma}$, we can see that a higher value of $\bar{\gamma}$ corresponds to a larger reduction in the success probability as we increase the tiers of interference T . This is because interference from distant levels becomes more significant at higher $\bar{\gamma}$. Furthermore, we see a saturation trend as we increase the value of T from 1 to 3, i.e., the reduction in success probability is more significant from $T = 1$ to $T = 2$ than from $T = 2$ to $T = 3$. Therefore, one can limit the tiers of interference to a finite value while doing outage analysis of such OLA network.

In Fig. 3, the results of average outage probability against SNR $\bar{\gamma}$ are depicted for different values of M and β . we see that at lower values of SNR, the network with lower M performs better because of reverse diversity effect, i.e., for low SNR, a smaller number of cooperating nodes, M , provides a lower outage probability, and vice versa. This is because for higher M , the low SNR cannot overcome the huge average path loss that exists between the transmitting and receiving nodes. Also, the path loss disparity is increased for higher M , which introduces an SNR penalty. However, for high SNR regime, the role of spatial diversity is evident for higher values of M . For instance, at $\bar{\gamma} = 15\text{dB}$ and $\beta = 2$, we can see 83%

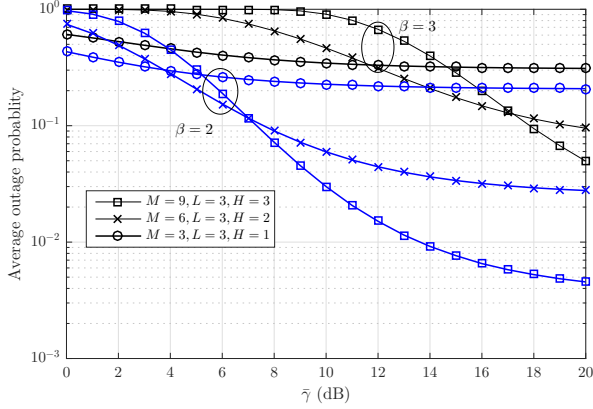


Fig. 3: The average outage probability versus $\bar{\gamma}$ for different values of M , L , H ; $d = 1m$, $T = 1$, $R = 1$, and $\tau = 0.2$.

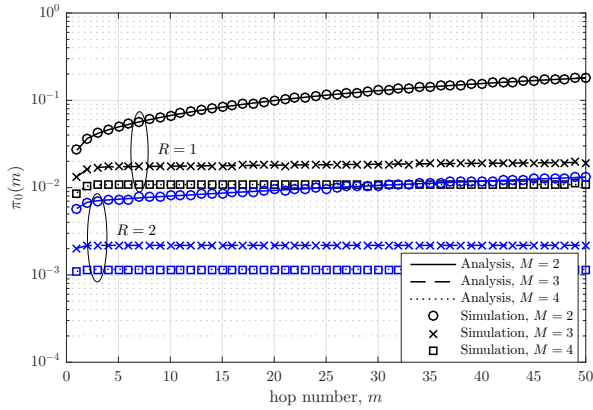


Fig. 4: The hop outage probability versus hop number m and for different values of M ; $d = 1m$, $L = 1$ and $H = M$, $T = 1$, $R = 1$, $\bar{\gamma} = 10\text{dB}$, $\tau = 0.1$, $\epsilon = 10^{-10}$, and $\beta = 2$.

and 77% decrease in outage as we increase M from 3 to 6 and 6 to 9, respectively. Similarly, the effect of β is interesting, i.e., if we compare two curves corresponding to $M = 9$, we can see that to have a 10% outage for $\beta = 3$, we need an extra SNR margin of 10dB compared to $\beta = 2$ case.

The hop outage $\pi_0(m)$, i.e., the probability of a hop being in an absorbing state, is depicted in Fig. 4 against the hop number m and for different values of R and M . We notice that the simulation and analytical results match closely, thereby verifying our Markov chain-based transmission model. It is worth-mentioning that Algorithm 1 converges after finite number of iterations, e.g., for $M = 4$ and $R = 1$, the algorithm converges in 23 iterations for $\epsilon = 10^{-10}$. It can also be observed that for a constant value of R , the hop outage is lower for higher values of M because of the spatial multiplexing and array gain. Moreover, the slope of the curves is seen to become smaller by increasing M indicating a slight degradation in the performance as the packets traverse the network. Also, the network with a higher value of R performs significantly better because the interfering levels are located farther from the receiving level for a higher value of R and offer larger path loss to desired level. However, the transmission rate also gets reduced by increasing R because of more idle slots.

In Fig. 5, the results of coverage distance against a required

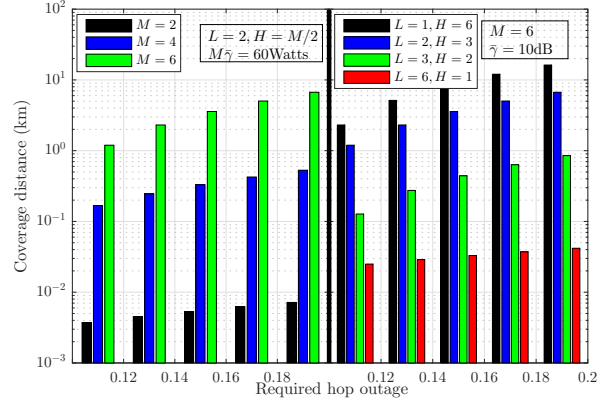


Fig. 5: The coverage distance versus required hop outage for different values of M , L , and H ; $d = 1m$, $T = 1$, $R = 1$, $\tau = 0.2$, $\epsilon = 10^{-10}$, and $\beta = 2$.

quality of service (QoS) are depicted for different values of M . The QoS is defined as the maximum value of the probability of hop outage. In other words, we require that the probability of a hop being in an absorbing state should be less than or equal to the required QoS. The total transmission power per hop is kept constant for all values of M for a fair comparison. It is evident in the figure that the coverage distance increases monotonically by increasing the required hop outage. The effects of spatial multiplexing is evident in Fig. 5, where coverage improves as M increases. Similarly, in the right half of Fig. 5, coverage distance versus QoS for different network topologies is plotted by varying values of L and H for a constant M . As we increase the value of L , the coverage distance is reduced because of higher average path loss for a large value of L . However, there is a trade-off between the latency of a network and transmission reliability, i.e., a large value of L corresponds to a bigger hop and thus a destination is reached using lesser number of hops. However, the average path loss of the system is large. On the other hand, a smaller value of L provides better reliability per hop, however, the latency of network increases as shorter hops will be made.

REFERENCES

- [1] R. I. Ansari and S. A. Hassan, "Opportunistic large array with limited participation: An energy-efficient cooperative multi-hop network," in *Proc. IEEE ICNC*, Feb. 2014.
- [2] W. Zheng and M. A. Ingram, "Maximum multi-hop range using cooperative transmission with a fixed number of nodes," *IEEE ICC*, June 2013.
- [3] B. Sirkeci-Mergen, A. Scaglione and G. Mergen, "Asymptotic analysis of multistage cooperative broadcast in wireless networks," *IEEE Trans. Inf. Theory*, vol. 52, no. 6, pp. 2531–2550, June 2006.
- [4] H. Jung and M. A. Weitnauer, "Multi-packet opportunistic large array transmission on strip-shaped cooperative routes or networks," *IEEE Trans. Wireless Commun.*, vol. 13, no. 1, pp. 144–158, Jan. 2014.
- [5] M. Hussain and S. A. Hassan, "Performance of multi-hop cooperative networks subject to timing synchronization errors," *IEEE Trans. Commun.*, vol. 63, no. 3, pp. 655–666, March 2015.
- [6] S. Talarico, M. C. Valenti, and T. R. Halford, "Unicast barrage relay networks: Outage analysis and optimization," in *Proc. IEEE Military Commun. Conf. (MILCOM)*, Oct. 2014.
- [7] S. Talarico, M. C. Valenti, and D. Torrieri, "Analysis of multi-cell downlink cooperation with a constrained spatial modelling," in *Proc. IEEE Global Commun. Conf. (GLOBECOM)*, Dec. 2013.